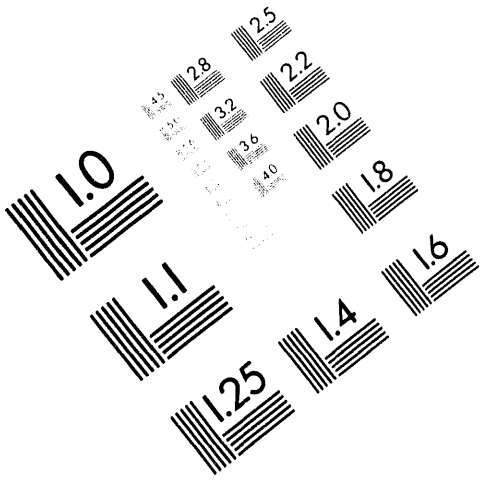

Association for Information and Image Management

1100 Wayne Avenue, Suite 1100
Silver Spring, Maryland 20910

301/587-8202

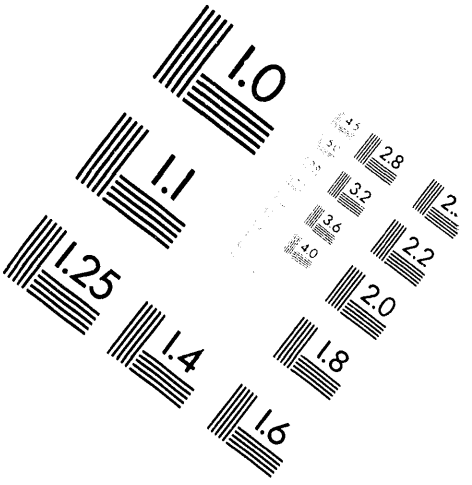

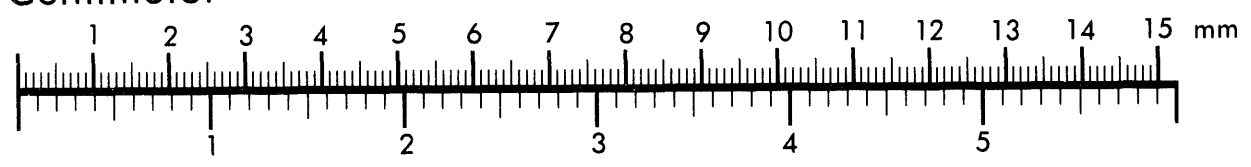

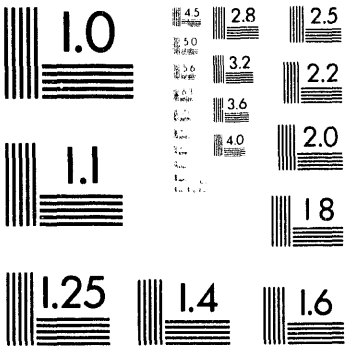

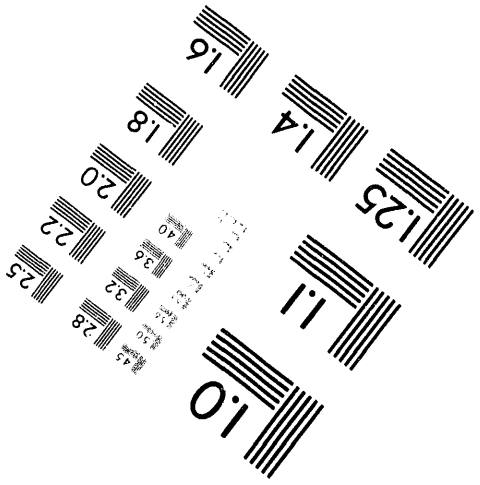

MANUFACTURED TO AIIM STANDARDS
BY APPLIED IMAGE, INC.

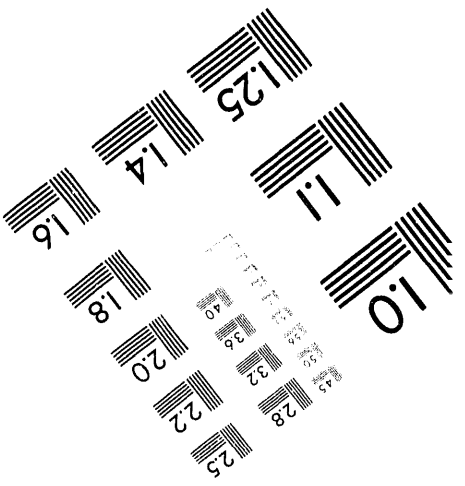

1 of 1

EROSION/REDEPOSITION ANALYSIS OF THE DIII-D DIVERTOR*

by

THANH Q. HUA AND JEFFREY N. BROOKS
Fusion Power Program
Technology Development Division
Argonne National Laboratory
Argonne, IL 60439 USA

May 1994

Submitted to the 11th International Conference on Plasma Surface Interactions in Controlled Fusion Devices, Joyo-Geibun Center, Mito-shi, Ibaraki-ken, Japan, May 23-27, 1994. (Sponsored by JAERI)

* Work supported by the United States Department of Energy/Office of Fusion Energy, under Contract No. W-31-109-Eng-38.

Erosion /Redeposition Analysis of the DIII-D Divertor*

T. Q. Hua and J. N. Brooks
Argonne National Laboratory
Argonne, IL 60439 USA

ABSTRACT

Carbon and tungsten sputtering and transport in the DIII-D divertor is analyzed with the impurity transport codes REDEP and WBC. Analysis is carried out for a recent DiMES experiment in which a carbon sample with a tungsten marker in the center was exposed to six well controlled ELM-free plasma discharges. WBC analysis predicts a high rate of ionization of tungsten neutrals within the sheath and subsequent redeposition on the DiMES sample. Qualitative comparison of the tungsten redeposited flux agrees well with measurements. REDEP analysis of net carbon erosion shows a factor of 2-3 agreement with measured data on the outboard side of DiMES and poor agreement on the inboard side.

* Work supported by the U.S. Department of Energy, Office of Fusion Energy, under Contract Number W-31-109-Eng-38.

1. Introduction

Erosion/redeposition has been an intense subject of investigation at DIII-D under the divertor material evaluation system (DiMES). The first phase of the study involved a long exposure test of twelve well characterized divertor carbon tiles. The tiles were exposed to about 1700 bottom divertor plasma discharges from March to December 1989. Comparisons were made between code predictions of carbon erosion/growth with experimentally measured profiles, [1]. Recent DiMES experiments, described in a companion paper [2], used samples which are 5 cm in diameter and were subject to a limited number of well controlled plasma discharges.

The present analysis focuses on the most recent experiment (commonly referred to as DiMES-8), conducted on October 21, 1994. In this test the carbon sample, which had a tungsten circle 1 cm in diameter vacuum deposited in the center, was exposed to six quiescent H-mode plasma discharges. The experiment was controlled such that ELM-free plasmas were maintained and the outer strike point was positioned as close as possible to the center of DiMES. For modeling, the impurity transport codes REDEP [3] and WBC [4] were used. WBC computes the transport of sputtered atoms and ions near a surface. The effects of the oblique magnetic field and sheath electric field are included, as are impurity-plasma interactions and Bohm diffusion. The REDEP code uses finite difference to solve iteratively a system of coupled integral equations governing hydrogen ion and neutral sputtering, self-sputtering, and redeposition, at discrete points on the divertor or limiter. Because of computer time limitations the WBC code is best suited for very detailed examination of a small region, such as the tungsten spot, while REDEP best treats the erosion/redeposition profile over the entire divertor surface. The two codes have thus been used in a complimentary manner for this analysis.

The companion paper [2] presents in detail post-exposure measurements of carbon erosion and redeposition on the graphite portion of DiMES and of tungsten erosion from the 1 cm marker and its redeposition elsewhere on the DiMES sample. Selected data is repeated in

this paper for comparison with code predictions. This comparison study is expected to benefit the codes through refinement of the existing model and identification of processes important to erosion/redeposition not included in the code. Just as importantly, valuable experiences will be learned for future tokamak in-situ erosion/redeposition experiments.

2. Modeling and Comparisons with Experiments

2.1 Carbon Erosion and Redeposition

The DIII-D divertor is completely covered with carbon tiles with the exception of a 1-cm diameter tungsten circle at the DiMES center. For the DIII-D plasma conditions most sputtered carbon atoms are ionized outside the magnetic sheath (see Table 2 and discussion in section 2.3), and subsequently return to the divertor surface at toroidal distances far from their sputtered origins. The absence of a primary carbon source at the tungsten spot would not have any significant effect on the carbon erosion profile on DiMES. Thus toroidal symmetry condition is assumed in global carbon erosion modeling.

Sputtering models used for the REDEP calculations are as follows. Deuterium ions and charge exchange neutrals impinge on the surface with average incidence angle (from the normal) of 60° and 45°, respectively. Charge exchange neutral flux equal to one quarter of the deuterium flux is assumed. Carbon neutrals that are ionized in the scrape-off layer return to the divertor with an average charge state +3 while carbon ions diffusing from the core are fully stripped of electrons. Average incidence angles of C^{+3} and C^{+6} ions are 60° and 50°, respectively. Sputtering coefficients of carbon are computed based on the DSPUT code model [5] for deuterium sputtering, and models in references [6,7] for self-sputtering. The sputtering coefficients are adjusted to better match results from the fractal-TRIM code [8]. Sputtered carbon neutrals are launched with an angular cosine distribution and velocity determined from

the random collision cascade model [9] for self-sputtering and from ITMC code calculations [10] for deuterium sputtering.

The REDEP code requires input plasma conditions to model the plasma at the near-surface region. Electron temperatures and densities used in this analysis were measured with a Langmuir probe located 2.8 cm radially outboard of the DiMES center, and at a different toroidal location from DiMES. The e-folding lengths of electron density and temperature are derived from that of heat flux recorded by an IR camera and assuming a relationship $\delta_T = 1.5\ \delta_n$, based on previous H-mode plasma profiles [1]. With these information, radial plasma profiles were constructed for input to the code. Table 1 summarizes the deduced plasma parameters.

As described in the companion paper [2], each shot in the DiMES-8 experiment consisted of two periods, averaging about 1 s in the first period and 1.5 s in the second period. The beam power was turned off for about 1 s between the two periods to maintain ELM-free discharges. Cumulative plasma exposure time of the DiMES-8 sample was approximately 13 seconds.

Strike point location was computed by the EFIT code [11] at 10 ms intervals, and the time-averaged location showed a small difference with that estimated from IR data. The normalized distributions of the strike point for all six shots are shown in Fig. 1, for both quiescent H-mode periods. EFIT also computes the total and poloidal magnetic field line angles which are 1.2° and 62° from the surface, respectively. The incident deuterium flux and sputtered and redeposited carbon flux are proportional to the total angle. The net erosion is strongly affected by the poloidal angle. In general a shallower poloidal angle will result in less local redeposition and higher peak net erosion.

The predicted net and gross erosion rates for period 1 are shown in Fig. 2. The gross erosion includes sputtering by deuterium, charge exchange neutrals, and self-sputtering of the redeposited carbon. The net erosion is the difference of gross erosion and redeposition. Redeposition reduces the peak erosion by a factor of 8. The redeposited carbon flux within ±2 cm of the strike point is about 95% of the sputtered flux, resulting in net erosion there. The integrated carbon flux over the calculation domain, however, approaches 98% of the sputtered flux, with 2% redeposition outside the area of interest. Eighty percent of the redeposited carbon ions are ionized in the near-surface layer, and twenty percent are ionized in the remaining scrape-off layer or core plasma.

For period 2, the computed gross and net erosion rate distributions (not shown) are similar to Fig. 2. The peak gross rate is about a factor of 2 higher as a result of higher deuterium, charge exchange neutral, and redeposited carbon fluxes, and higher sputtering coefficients. The peak net erosion rate is 2.2 nm/s.

The integrated carbon erosion profile was determined by (1) convolving the computed net erosion rates with the time-averaged strike point distributions, and (2) multiplying the rates by the plasma exposure time. The computed profile is compared to carbon erosion measurements [2] along the radial scans on the probe. The predicted erosion on the probe is higher on the outboard side than the inboard side while Rutherford Backscattering (RBS) analysis [2] of the sample shows a reverse trend. The predicted net erosion agrees with measured erosion within a factor of 2-3 along the outboard scans but shows poor agreement along the inboard scans.

The discrepancies between REDEP analysis and measurements warrant further investigation/improvement of the models, and the accuracy and availability of the measured plasma parameters. For example, in previous erosion modeling of the DIII-D divertor [1], a possible mechanism which resulted in net transfer of sputtered material from the outer strike

point region (location of DiMES) to the inner strike point region was identified. Such an analysis was not pursued here because of insufficient plasma data to model the inner strike point region. A rigorous study also requires better characterization of the plasma parameters and profiles than those available for this analyses. Improved modeling of plasma density and temperature in the scrape-off layer may be needed for the DIII-D plasma regime (present analysis assumes constant density and temperature along a poloidal field line). Further analysis is planned for the future.

2.2 Tungsten Sputtering and Transport

The WBC code computed the sputtering of tungsten atoms from the 1 cm diameter tungsten spot, and the subsequent ionization, transport, and redeposition of tungsten ions to the entire 5-cm diameter DiMES probe. For the measured plasma conditions, i.e., with peak electron temperature T_{eo} = 30 eV, and an assumed average D^+ impact energy of U_o=150 eV, there is no predicted sputtering of tungsten by the deuterium ions. All tungsten sputtering is therefore due to impinging carbon ions, self- sputtering, plus any trace impurities. The carbon flux arises mostly from the rest of the carbon divertor and a small contribution from plasma sputtering of the graphite portion of DiMES. The REDEP analysis was used to determine the carbon fiux to the tungsten spot. For the present analysis, a particle history terminates upon returning to the divertor surface. The subsequent re-sputtering of redeposited material was not followed, and is believed to be a second order effect for the short DiMES exposure times.

For the simulation, 300,000 tungsten atoms are launched from the surface with an energy distribution supplied by the ITMC binary-collision-model sputtering code [10] for 250 eV C on W. The latter value is the predicted average energy of redeposited carbon ions. A "cosine" type elevation angle distribution and uniform azimuthal distribution were used. The computed profile of redeposited tungsten is qualitatively compared to the measured areal density of Wampler et al. [2] for the toroidal direction, Fig. 4 , and the radial direction, Fig. 5. It is assumed for this

comparison that the measured tungsten concentration is proportional to the redeposited flux. Using this assumption, the data is normalized to the computed flux at one point (first data point of curve E in Fig. 4), and the rest of the data is rescaled by the same normalization factor.

The comparisons show good agreement for the parallel field transport, Fig. 4, showing trends of: (1) more deposition downstream than upstream, and (2) an exponential fall-off of the redeposition with distance. The agreement with the radial scans is good for the near sample region but the data shows more apparent radial transport at farther distances than the code predicts (both for Fig. 5 and other scans not shown). An attempt was made to identify possible reasons for the higher radial transport. The following variations or additions to the code were found not to result in a significantly better match with data : (1) a pre-sheath electric field, (2) a radial electric field, and an increase (x5) in particle diffusion coefficient.

Another point of comparison is the absolute erosion of the tungsten spot. This comparison is made quite difficult because of possible formation of a carbon overlayer on to the tungsten surface. This carbon layer, if it exists, would substantially reduce the tungsten sputtering, and was not accounted for in the present analysis. Such an overlayer can arise from transfer of carbon from the surrounding carbon areas onto the tungsten spot. A thick buildup of carbon on tungsten is not expected, as discussed in section 2.1, since the DiMES center is in the region of net carbon erosion. However a very thin (1-5 nm) carbon film may exist before pseudo-equilibrium is obtained between deposited carbon and D^+ etc. sputtering of carbon. Such an effect was observed in the PISCES molybdenum transport experiment [12], and in ASDEX [13]. As shown by ITMC calculations for the PISCES experiment [12], the presence of a 1-3 monolayer thick carbon film can greatly suppress the sputtering of molybdenum, and this is expected for tungsten as well.

RBS analysis of the post-tokamak exposure DiMES 8 probe [2] ruled out a thick (>5 nm) carbon layer on the tungsten, but the RBS technique is not capable of detecting monolayer coverage. Further analysis of the sample is planned [14].

If a carbon overlayer is neglected, the predicted tungsten gross erosion (sputtering only) and net erosion (sputtering minus redeposition) are 16.2 nm and 3.1 nm, respectively. This is based on the predicted fluxes of carbon ions and redeposited tungsten ions, sputtering coefficients for C and W on the as-prepared tungsten material (70% .at W, 15 .at% C, 15 .at% 0), and the plasma exposure time of 13.5 s. The net tungsten erosion of 0.7 nm inferred from the material redeposited on the sample outside the marker was a factor of 5 lower than predicted. The difference may be, and is likely, due in part to a carbon overlayer. If not, this suggests substantial errors/disparities in the plasma measurements and/or calculations.

2.3 Comparison Among Tungsten, Carbon and Beryllium

To help plan future experiments, analysis was carried out for 1 cm diameter circles of carbon and beryllium using the same plasma conditions of DiMES 8. Table 2 summarizes the simulation results for all three materials. A key difference between tungsten and low-Z materials is the much shorter mean free path for neutral ionization. As discussed in detail in [4,15] the sputtered tungsten atoms are much more likely to be ionized within the magnetic sheath region, for tokamak divertor conditions. Subsequent tungsten ion transport to the surface is faster and more localized because of the strong electric field in the magnetic sheath. In contrast, sputtered atoms ionized outside the sheath (including some of the tungsten) depend primarily on the slower process of collisional friction with the incoming sound-speed-flowing plasma for redeposition. As shown in Table 2, almost all of the sputtered tungsten is redeposited on the 5 cm diameter probe surface, in contrast to about 25% for carbon and beryllium. (This parameter should not be confused with the carbon redeposition fraction over the entire divertor surface which does approach 100%).

3. CONCLUSIONS

This work has continued the important activity of erosion/redeposition code benchmarking by analyzing the DiMES-8 limited-exposure experiment. Both carbon and tungsten sputtering and redeposition on the divertor probe have been computed and compared to experimental data. Although the work has been constrained by the very limited probe-region plasma data available, it has been possible to make several encouraging comparisons/conclusions.

For both materials, a key prediction of the models is that the net erosion rate is an order of magnitude lower than the gross rate. The present results for carbon are consistent with this prediction, showing a factor of ~2-3 agreement between the measured and predicted peak net erosion on the outboard side of the DiMES sample. The predicted erosion profile, however, differs significantly from the measured one. This may be due to differences in strike point locations, plasma profiles, and magnetic field geometry, from the ones used in the simulations. Transfer of material to/from the inner divertor and first wall, is another possibility, which we plan to analyze further.

A key modeling result for tungsten is the prediction of substantial in-sheath ionization of the slow-moving sputtered atoms, and a consequently high local redeposition rate. The computed redeposition profiles for tungsten, in the surrounding carbon, match well with the profiles inferred from the measurements, thus tending to confirm the model. The comparison of absolute erosion for tungsten is made difficult because of the likely presence of a carbon overlayer. Another point of comparison is that the code predicts that essentially no sputtered tungsten leaves the near-surface plasma - this is consistent with the lack of core plasma tungsten

found in the experiment. Both these results, and the results for tungsten in ASDEX [13] appear favorable for considering tungsten as a plasma facing material candidate.

REFERENCES

[1] C.P.C. Wong, et al., J. Nucl. Mater., 196-198 (1992) 871.

[2] R. Bastasz et al., these proceedings.

[3] J.N. Brooks, Nucl. Technol./Fusion 4 (1983) 33.

[4] J.N. Brooks, Phys. Fluids 8 (1990) 1858.

[5] D.L. Smith, et al., Proc. 9th Symp. Engineering Problems of Fus. Res., IEEE Pub. #81CH1715-2 (1981) 719.

[6] N. Matsunami et al., At. Data Nucl. Data Tables 31 (1984) 1.

[7] Y. Yamamura, Y. Ytikawa, and N. Itoh, IPPF-AM-26 (Inst. Plas. Phys. Nagoya Univ. 1983).

[8] J.N. Brooks and D.N. Ruzic, J. Nucl. Mater. 176&177 (1990) 278.

[9] N. Thompson, Philos. Mag. 18 (1968) 377.

[10] A.H. Hassanein and D.L. Smith, J. Nucl. Instr. Meth. Phys. Res., B 13 (1986) 225.

[11] L.L. Lao et al., Nucl. Fusion 30 (9190) 1035.

[12] M.J. Khandagle et al., J. Nucl. Mater. 207 (1993) 116.

[13] D. Naujoks et al., "Erosion and Redeposition is the ASDEX Upgrade Divertor," J. Nucl. Mater., to be published.

[14] W.R. Wampler, private communication (1994).

[15] J.N. Brooks in Atomic and Plasma Material Interaction Processes in Controlled Thermonuclear Fusion, R.K. Janev and H.W. Drawin, Editors, Elsevier (1993) 403.

Figure Captions

1. Time-averaged distribution of the outer strike point location inferred from MHD reconstruction of the plasma flux geometry relative to the DiMES probe whose center is at r=148.6 cm.

2. The REDEP computed gross and net erosion rates for the period 1 plasma conditions.

3. Comparison of the measured carbon erosion/deposition on DiMES with REDEP predictions. Measurements were taken along radial scans crossing the probe diameter (M), upstream (U), and downstream (D). The U and D scans are offset by 7 mm from the centerline.

4. Comparison of WBC code predictions of the normalized tungsten redeposition profiles with measurements for the toroidal scans.

5. Comparison of WBC code predictions of the normalized tungsten redeposition profile with the measured data along the radial scans. The scans are offset by 7 mm from the radial centerline.

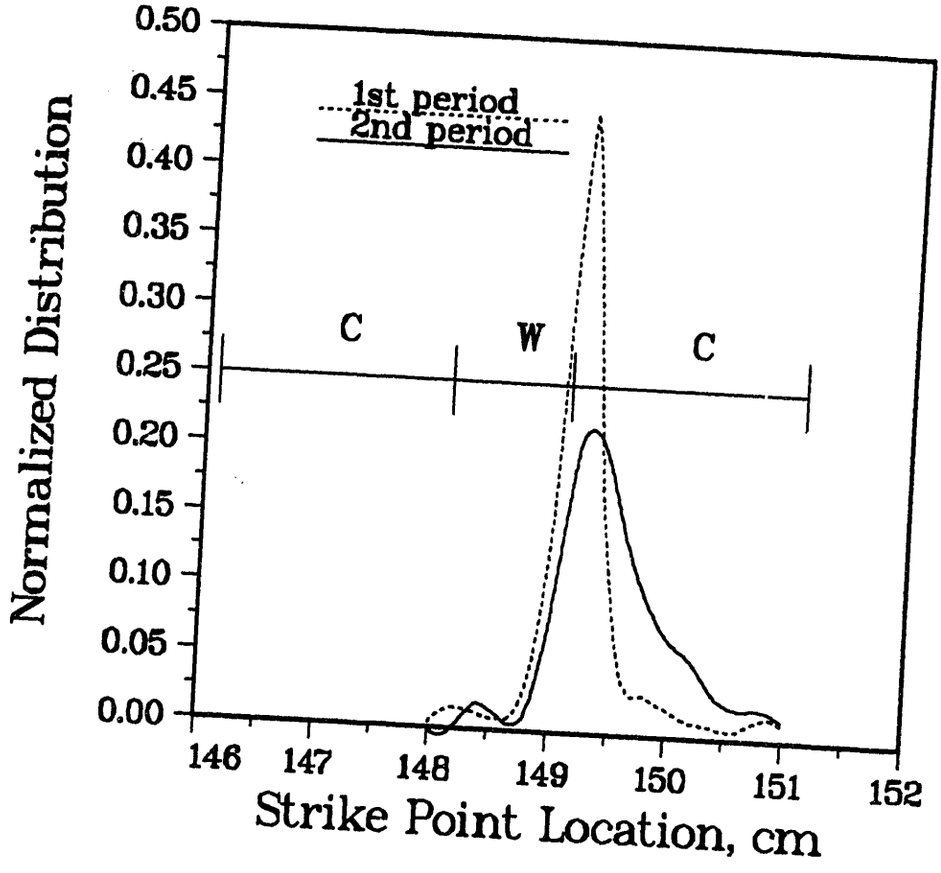
0.50
0.45
0.40
0.35
0.30
0.25
0.20
0.15
0.10
0.05
0.00
Normalized Distribution
1st period
2nd period
C
W
C
146
147
148
149
150
151
152
Strike Point Location, cm

Fig. 1

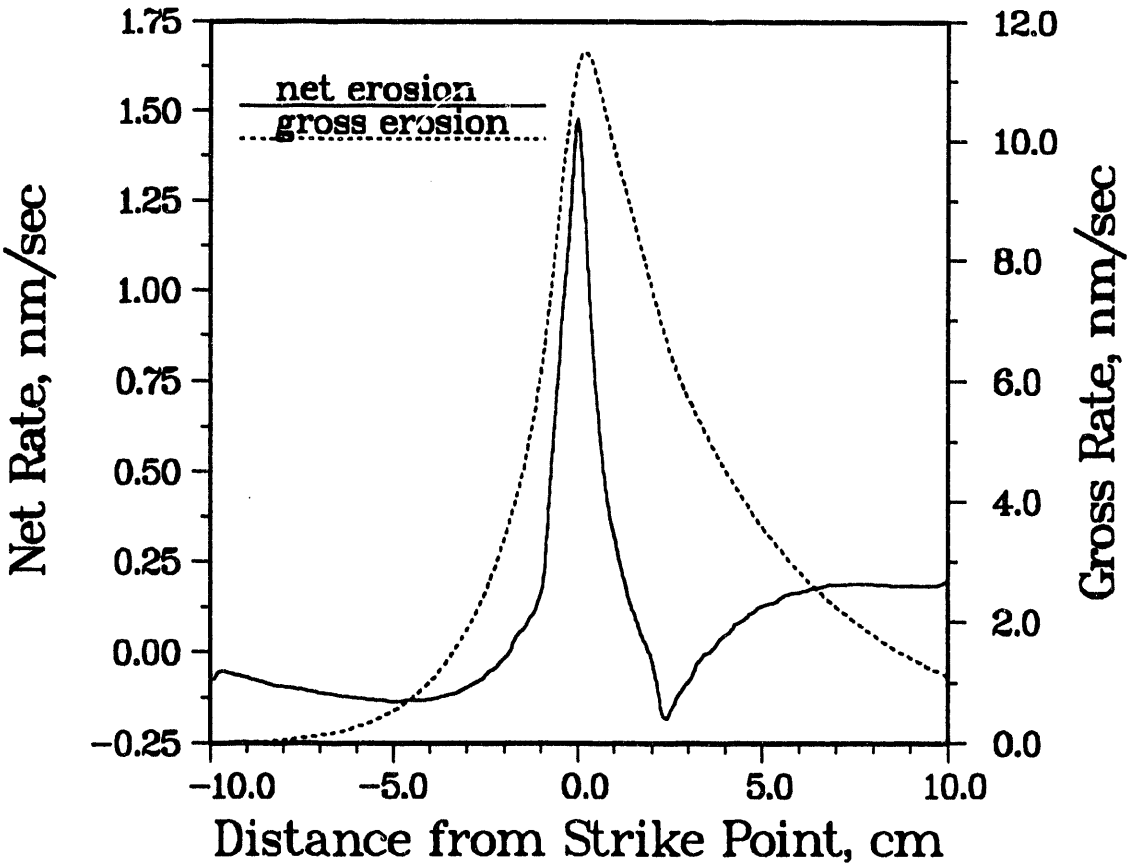
net erosion
gross erosion
Net Rate, nm/sec
Gross Rate, nm/sec
Distance from Strike Point, cm
1.75
1.50
1.25
1.00
0.75
0.50
0.25
0.00
-0.25
12.0
10.0
8.0
6.0
4.0
2.0
0.0
-10.0
-5.0
0.0
5.0
10.0

Fig. 2

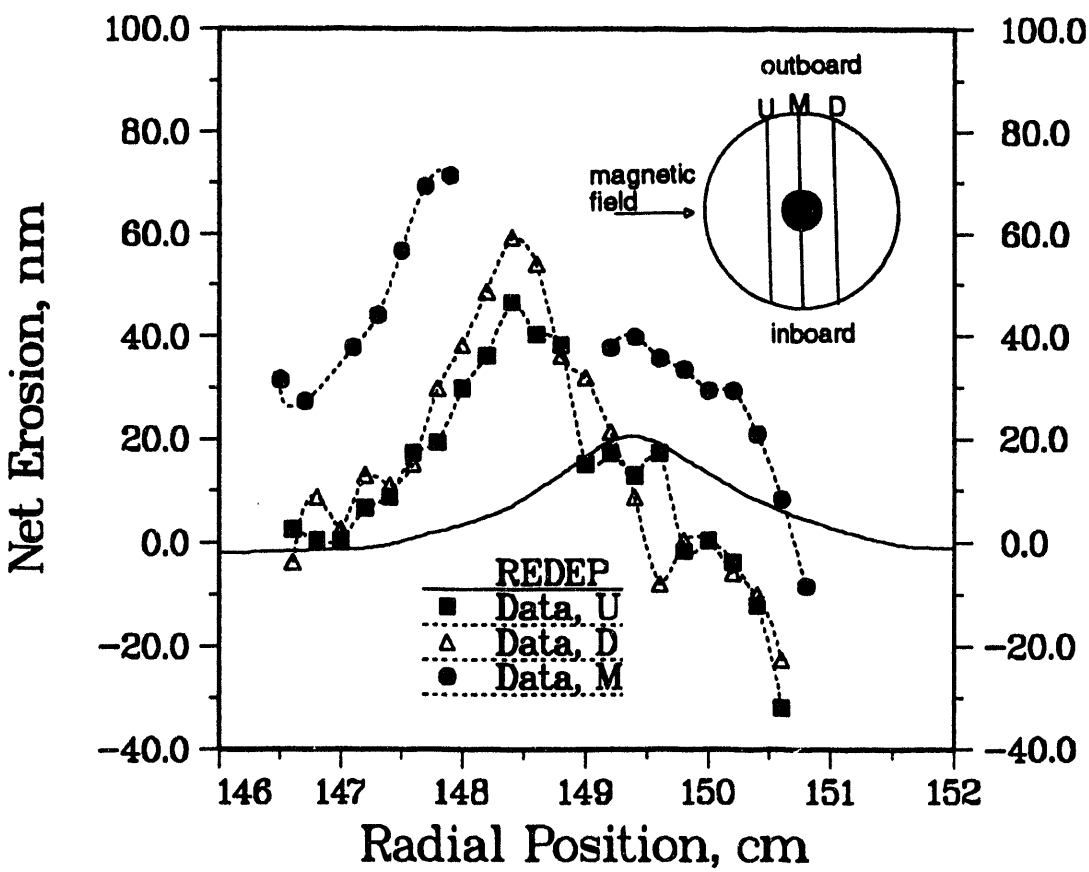
100.0
80.0
60.0
40.0
20.0
0.0
-20.0
-40.0
Net Erosion, nm
outboard
U M D
magnetic field
inboard
REDEP
Data, U
Data, D
Data, M
146
147
148
149
150
151
152
Radial Position, cm

Fig. 3

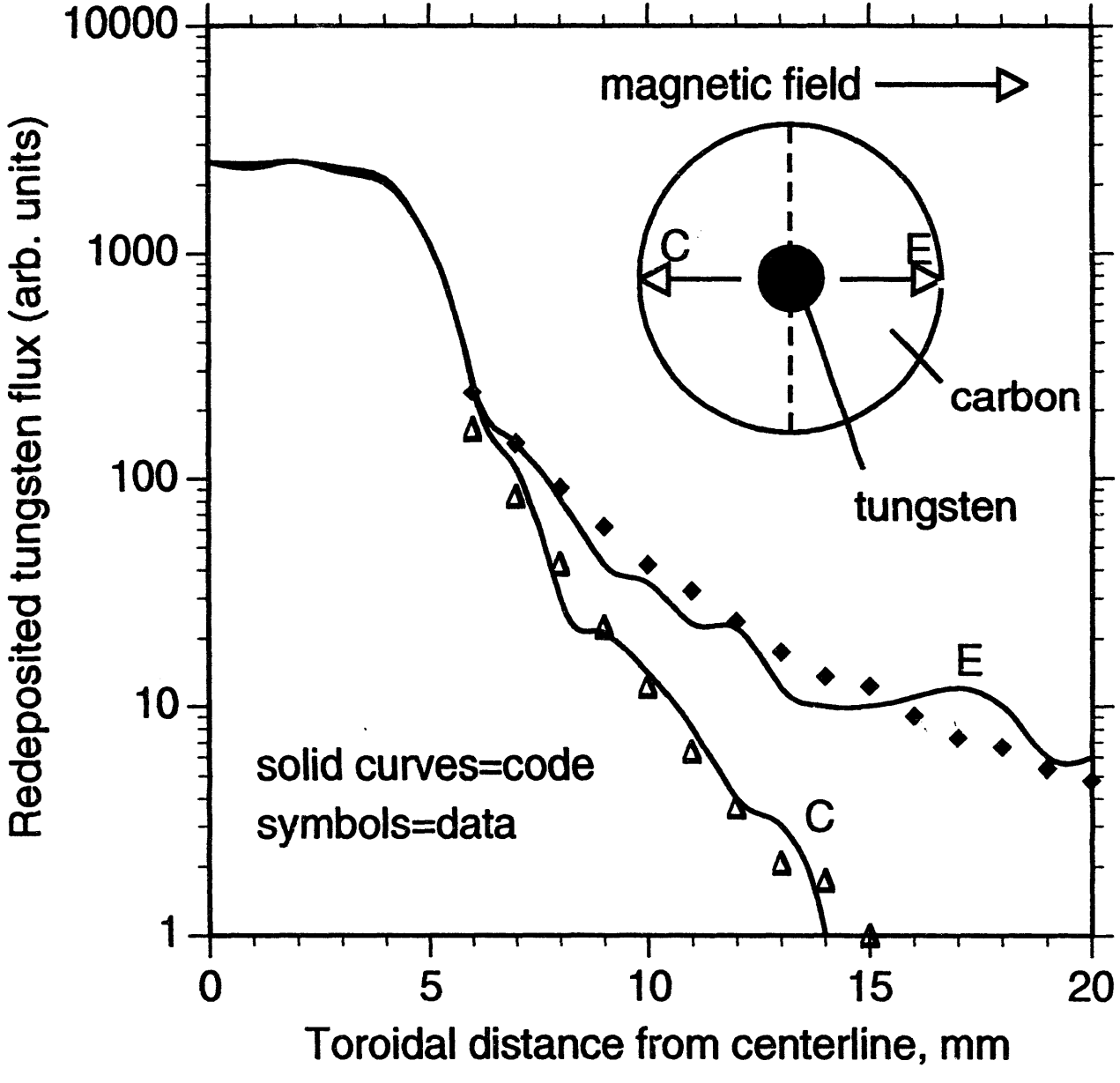
10000
1000
100
10
1
Redeposited tungsten flux (arb. units)
magnetic field
C
E
carbon
tungsten
E
C
solid curves=code
symbols=data
0
5
10
15
20
Toroidal distance from centerline, mm

Fig. 4

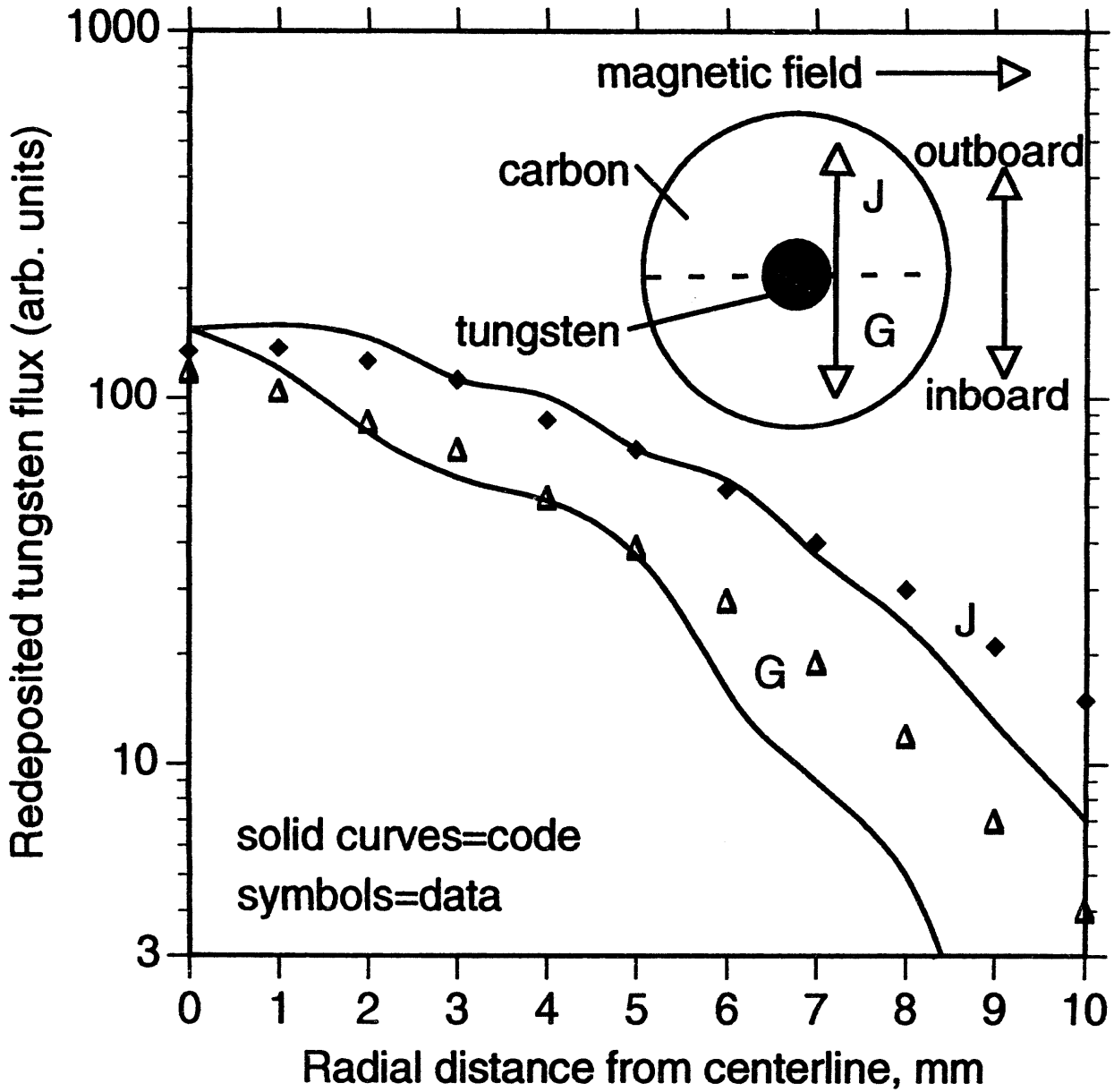
1000
100
10
3
Redeposited tungsten flux (arb. units)
magnetic field
carbon
tungsten
J
G
outboard
inboard
J
G
solid curves=code
symbols=data
0
1
2
3
4
5
6
7
8
9
10
Radial distance from centerline, mm

Fig. 5

Table 1. Input Plasma and Magnetic Field Parameters for REDEP Analysis

		Period 1	Period 2
Peak electron temperature,	T_{eo} (eV)	23.6	29.5
Peak electron density,	n_{eo} ($x10^{19}$ m^{-3})	1.9	2.4
Temperature e-folding lengths,	δ_{TR} (m)	0.144	0.144
	δ_{TL} (m)	0.054	0.054
Density e-folding lengths,	δ_{nR} (m)	0.096	0.096
	δ_{nL} (m)	0.036	0.036
Total field angle,	θ_T (°)	1.2	1.2
Poloidal field angle,	θ_p (°)	62	62

*Subscript R means to the right of the strike point, L means left.

Table 2. Summary of impurity transport parameters -- WBC code simulation of DiMES-8 tungsten, and hypothetical carbon and beryllium experiments, $n_{eo} = 3 \times 10^{19}$ m^{-3}, $T_{eo} = 30$ eV, $\alpha = 1.2°$.

Parameter*		Tungsten	Carbon	Beryllium
Neutral ionization distance, mm (perp. to surface)	$\bar{z}_o$	.59	8.4	5.8
Charge state	$\bar{K}$	1.8	2.1	1.7
Ion transit time, μs	$\bar{\tau}$	.97	15	12
Elevation angle, °	$\bar{\theta}$	15	51	51
Energy, eV	$\bar{U}$	146	256	197
Redeposition fraction				
on sample (1 cm dia.)	f_1	.79	.13	.15
on entire DiMES probe (5 cm dia.)	f_5	.97	.25	.30

*Bar denotes average for redeposited particles.

DATE

FILMED

7/14/94

END